


Dosimetric Effect of Intrafraction Tumor Motion in Lung Stereotactic Body Radiotherapy Using CyberKnife Static Tracking System

Technology in Cancer Research & Treatment
 Volume 18: 1-10
 © The Author(s) 2019
 Article reuse guidelines:
sagepub.com/journals-permissions
 DOI: 10.1177/1533033819859448
journals.sagepub.com/home/tct


Yu Chang, PhD¹, Hong-Yuan Liu, MS¹, Zhi-Wen Liang, MS¹,
 Xin Nie, PhD¹, Jing Yang, PhD¹, Gang Liu, PhD¹ , Qin Li, MD¹,
 and Zhi-Yong Yang, PhD¹ 

Abstract

Purpose: We investigated the dosimetric effect of intrafraction tumor motion in lung stereotactic body radiotherapy using the CyberKnife static tracking system. **Methods:** Four-dimensional computed tomography scans of a dynamic thorax phantom were acquired. Two motion ranges, 3 collimator sizes, and 4 treatment starting phases were investigated. Monte Carlo dose distributions were calculated on internal target volume with a treatment-specific setup margin for 6 Gy/1 fraction. Dosimetric effects of intrafractional tumor motion were assessed with Gafchromic films. γ (5%/3 mm), dose differences, and distance to agreement were analyzed. **Results:** With 30 mm collimator plans, the measured dose passed the criteria γ (5%/3 mm) in all tumor motion ranges. The γ passing rates of the plans using 20 mm or 20+35 mm collimators were much lower than that with 30 mm collimator, especially with the 30 mm tumor motion range. The measured dose of 10 mm tumor motion ranges all passed the 90% criteria of γ (5%/3 mm), the results being much better than those of 30 mm tumor motion ranges, which were below 80%. The results of same delivered plan but treated with different starting phases varies greatly. **Conclusion:** Xsight Lung Tracking technique should be used with caution in lung cancer stereotactic body radiation therapy because the temporal dose variations can be significant.

Keywords

4DCT, CyberKnife, spine tracking, SBRT, respiratory motion

Abbreviations

AVP, average-intensity projection; DD, dose difference; DTA, distance to agreement; GTV, gross tumor volume; IMRT, intensity-modulated radiation therapy; ITV, internal target volume; MIP, maximum-intensity projection; PTV, planning target volume; SBRT, stereotactic body radiation therapy; SI, superior–inferior; TPS, treatment planning system; XST, Xsight Spine tracking; 4DCT, 4D computed tomography

Received: January 07, 2019; Revised: April 01, 2019; Accepted: May 22, 2019.

Introduction

The treatment of tumors in motion is particularly challenging when delivering high-dose hypofractionated treatments such as stereotactic body radiation therapy (SBRT). The CyberKnife Robotic Radiosurgery System (Accuray Inc, Sunnyvale, California) has been increasingly employed for SBRT of lung cancers, as it offers various ways, such as Xsight Lung Tracking, fiducial tracking, and Xsight Spine tracking (XST), to locate and track the tumor in different anatomical regions. Xsight Lung Tracking is most suitable for tumors with a large moving

range, located in the lung and upper abdomen because of the gain in safety margin reduction.¹ For the visualization of

¹ Cancer Center, Union Hospital, Tongji Medical College, Huazhong University of Science and Technology, Wuhan, China

Corresponding Author:

Zhi-Yong Yang, Cancer Center, Union Hospital, Tongji Medical College, Huazhong University of Science and Technology, Wuhan 430022, China.
 Email: yang_zhiyong@hust.edu.cn



tumors that are sheltered by bone anatomy or central organs, an implanted fiducial is necessary to correctly identify the target in the projection x-ray images.² However, some patients are not suitable to undergo percutaneous transthoracic fiducial insertion due to the associated risk of complications, including pneumothorax, pulmonary hemorrhage, air embolism, and fiducial migration.³ For tumors that are near to or attached to the skeletal structures and have a small range of motion, XST, a static tracking method utilizing the alignment of the spinal skeleton structure, could also be used.^{4,5} This treatment setting strategy is conceptually consistent with the recently available lung optimization treatment option 0-view tracking mode, which utilizes XST of adjacent vertebral bodies for global patient alignment.⁶

Since the XST and 0-view tracking modes are not real-time tumor motion tracking methods, and do not account for the uncertainty of the interfractional and intrafractional of the tumor motions, it is necessary to include the entire trajectory of the target motion into the treatment volume. According to International Commission on Radiation Units and Measurements (ICRU) report 62, the internal target volume (ITV) is drawn by 4D computed tomography (4DCT) images, or, in less than ideal cases, by breath holding CT imaging at the end of inspiratory and end of expiration of the normal breathing.⁷ The planning target volume (PTV) is designed to cover the source of all geometric errors by expanding the ITV, such as setup errors, random movements of the patient, and changes in respiratory motion.

Since XST requires an ITV to account for respiration-induced organ motion, motion effects on the tumor dose cannot be neglected. These effects can be broadly divided into the gradient effect, which causes the dose blurring, and the interplay effect.^{8,9} While a large number of small photon beams are combined to dose-paint the tumor volume during CyberKnife treatment, the dose delivered to each voxel of the tumor may not add up to its expected total dose because the tumor moves in and out of the radiation fields with respiratory motion. The interplay effect between tumor motion and complex collimator movement also compromises dose accuracy during CyberKnife treatment for a moving target, creating hot, and cold spots within the target, which cannot be resolved by adding margins.⁹ For homogeneously irradiated target volumes, such as conformal and intensity-modulated radiation therapy (IMRT), the interplay effect could be defined as any deviation between the tumor dose at the planned value and in the case of dynamic delivery and tumor movement. However, due to the inhomogeneous dose distribution of SBRT plan, it is more challenging to distinguish the gradients and interplay effects in dynamic deliveries experiments. Since the gradient effect is purely spatial, and the interplay effect has an additional temporal component, the logical method of separating the interplay effect is to analyze the dosimetric deviations of the different starting phases of the motion relative to the beam start time.⁹ Bortfeld *et al* suggested that the interplay effect tends to average with the large number of treatment fractions.⁹ However, this is not automatically applicable to hypofractionated SBRT (1-5 fractions). The dosimetric impact of intrafractional target motion has been experimentally

investigated in conventional linac-based isocentric irradiation by Richter *et al* for single beam,¹⁰ by Nakamura *et al* and Huang *et al* for coplanar and noncoplanar conformal radiotherapy,^{11,12} by Jiang *et al* and Chen *et al* for IMRT,^{8,13} and Riley *et al* for volumetric arc radiotherapy.¹⁴ Chan *et al* have performed experimental investigations of the intrafractional target motion during CyberKnife treatment, focusing on real-time tracking and XST.¹⁵⁻¹⁷ However, the influence of beam sizes and that of the interplay effect have not been experimentally studied.

In this study, we aimed to quantitatively evaluate the interplay effects of tumor motion and the adequacy of using an XLS-based strategy to treat a moving tumor. We tested the dose deviations of different combination of collimator sizes, tumor motion ranges and periods, the prescription doses, and treatment starting phases of the delivery plans. Experimental dose measurements were made with Gafchromic EBT3 films placed inside a thorax phantom with a moving tumor substitute.

Materials and Methods

Motion Phantom Setup

The dynamic QUASAR phantom (Modus Medical Devices Inc, Ontario, Canada) used in this experimental study consisted of a moving spherical target with film inserts that can accommodate Gafchromic EBT3 films (Ashland Inc, Wayne, New Jersey) in coronal plane, as shown in Figure 1. The tumor substitute was a 30-mm diameter sphere with density of 1.06 g/cm³ that was embedded in a cylindrical lung insert made of low-density cedar (0.4 g/cm³). The phantom was programmed to move the target in periods of 3 or 5 seconds and at variable ranges: (1) 10 mm in the superior-inferior (SI) direction and (2) 30 mm in the SI direction. The maximum distance between the target's center and the phantom's substitute spine was 7 cm. Constant motion was assumed in 4DCT simulation and treatment deliveries.

4DCT Simulation, Target Definition, and ITV-to-PTV Margin Determination

The 4DCT images of 1.5 mm thickness were acquired on a Philips Brilliance Big Bore CT simulator (Philips Healthcare, Netherlands) together with the real-time position management system (Varian Medical Systems, Palo Alto, California). For each 4DCT data set, 10 equally time-binned 3-dimensional computed tomography (3DCT) data sets were created, with the 0% image data set and the 50% image data set roughly corresponding to the end of inhalation and end of exhalation phases in the respiratory cycle, respectively. Additionally, 2 reconstructed data sets using maximum-intensity projection (MIP) and average-intensity projection (AVP) were also created. Both MIP and AVP created 3DCT images represented the greatest and average voxel intensity values throughout the 4DCT data set, respectively. Both the MIP and the AVP data sets were imported into the Multiplan v. 5.2 (Accuray Inc) treatment planning system (TPS). The ITV was produced as the union of gross tumor volume (GTV) over the motion trajectory on the

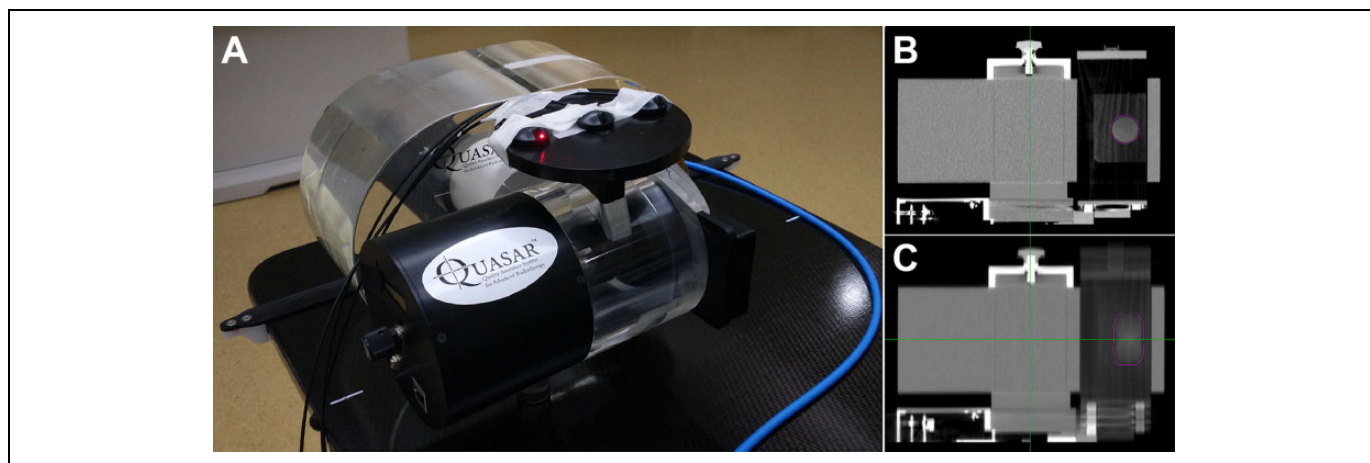


Figure 1. The dynamic thorax phantom (A) and coronal plane CT images of midventilation phase (B) and AVP (C). The PTV contour is also shown in the AVP images (C). AVP indicates average-intensity projection; CT; computed tomography; PTV, planning target volume.

Table 1. Summary of the Plan Delivered and the Active Motion Parameters in Measurements.

Measurement #	Plan #	Delivered Plan			Motion and Measurement Parameters		
		Collimator, Φ (mm)	Prescription (%)	Length of ITV in SI Direction (mm)	Range (mm)	Periods (seconds)	Phase of Treatment Start
M1(1,2) ^a	P1	20	60	40	10	5	Exhale
M2(1,2)	P2	30	60	40	10	5	Exhale
M3(1,2)	P3	20 + 35	60	40	10	5	Exhale
M4(1,2)	P4	20	60	60	30	5	Exhale
M5(1,2)	P5	30	60	60	30	5	Exhale
M6(1,2)	P6	20 + 35	60	60	30	5	Exhale
M7(1,2)	P5	30	60	30	Static	NA	Mid
M8(1,2)	P5	30	60	60	30	5	Mid(Exhale-Inhale)
M9(1,2)	P5	30	60	60	30	5	Mid(Inhale-Exhale)
M10(1,2)	P5	30	60	60	30	5	Inhale
M11(1,2)	P7	30	75	60	30	5	Exhale
M12(1,2)	P8	30	60	60	30	3	Exhale

Abbreviations: ITV, internal target volume; SI, superior–inferior.

^aM1(1,2) means the M1group was measured twice.

MIP images. Margins from the ITV to the PTV were 4.5 mm, as using the margin recipe of Descovich *et al* and our previous study of the Xsight Lung treatment of CyberKnife, which a 4.5 mm ITV-to-PTV in all 3 directions is enough to cover 95% GTV over entire fractions.^{4,18}

Treatment Planning

Multiplan v. 5.2 was used for treatment planning. In the XST mode, a region of interest that included a substitute spine volume of the phantom at a less than 7 cm distance from PTV was defined. For each motion profile, we performed Monte Carlo dose optimization on the AVP images using different collimators, as suggested by previous studies^{17,19}: one of a dimension that is smaller than the planning ITV (20 mm), one with a dimension that matches the ITV's short axis (30 mm), and a combination of a dimension that is larger than the planning ITV's short axis (35 mm) plus a dimension that is smaller than the planning ITV (20 mm). All Monte Carlo dose calculations

were performed at 0.5% relative statistical uncertainty. The dose grid resolution was approximately 1.0 mm \times 1.0 mm \times 1.5 mm. Dose distributions were Gaussian-smoothed to reduce statistical noise. Total doses of 6 Gy in 1 fraction were prescribed to 60% or 75% isodose lines (maximum dose = 100%) to achieve >99% target coverage. Table 1 presents a summary of the final treatment plans.

Treatment Setup and Delivery

Treatment setup was performed with the XST by CyberKnife VSI system (Accuray Inc). In brief, the phantom loaded with the EBT3 films was placed on the treatment couch, then x-ray image pairs of the substitute spinal column were acquired and compared with digitally reconstructed radiographs (DRRs).⁵ The registration errors were subsequently corrected by moving of the treatment couch until the setup errors were reduced to less than 0.5 mm (translational) and 0.5° (rotational). The residual error for the spine alignment was then corrected by the CyberKnife robot, and

the treatment beams were delivered to the moving target according to the spine–tumor relationship from the planning CT. In order to analyze the interplay effects of the treatment starting phases, 4 treatment starting phases were chosen to be measured: (1) end of exhale (Exhale); (2) midventilation: from exhale to inhale (Mid[Exhale-Inhale]); (3) end of inhale (Inhale); and (4) midventilation: from inhale to exhale (Mid[Inhale-Exhale]). The different treatment plans were measured with different phantom motion parameters twice for the statistical error. The film analysis results were compared and determined the interplay effect induced by the different treatment starting phases.

Film Analysis

We used an Epson Expression 1000XL flatbed scanner (Epson America, Long Beach, California) to scan the EBT3 films within 24 hours postirradiation with the following settings: (1) transmission mode, (2) 48-bit color (RGB), (3) resolution of 150 dpi (0.017 cm/pixel), (4) no color correction, and (5) portrait orientation. Each exposed film was scanned 3 times and averaged to reduce the scanner electronic noise. The EBT3 films were calibrated by measurements with an ion chamber and corrected with the OmniPro-I^mRT software (OmniPro-I^mRT 1.7, IBA dosimetry, Germany). Absolute film dosimetry has been reported to show good results in dose measurements and quality assurance of CyberKnife radiotherapy.^{20,21} The film dose distribution was registered to the dose plane exported from the Multiplan TPS. The films were compared to the calculated dose based on the global γ metric, which aims to quantitatively compare the measured and calculated dose distributions by dose differences (DD) and distance to agreement (DTA). In principle, the γ criteria should be set in accordance to the desired dosimetric accuracy of the treatments. Considering the dose uncertainty of EBT3 film dosimetry and the increased sensitivity of measurement errors to the large dose gradient of SBRT, the initial passing criteria γ (5%/3 mm) were set at 5% of the absolute DD and 3-mm DTA with low-dose threshold of 10%, assuming a 1-mm error in residual tracking accuracy and a 2-mm error associated with the film alignment during measurement and image registration between film and dose plane during analysis.¹⁶ Then, 3%/3 mm criteria and 2%/2 mm criteria (assuming a 1-mm error in residual tracking accuracy and a 1-mm error associated with the film alignment during measurement and image registration between film and dose plane during analysis) were also analyzed as recommended in the AAPM report 135 for quality assurance of robotic radiosurgery.²² The 5% or 3% of the absolute DD and DTA 3 mm criteria were also analyzed. We further considered the acceptance level of the percentage of pixels passing the γ (5%/3 mm) to be $\geq 90\%$.

Results

γ Analysis Results Between Different Collimator Sizes

Table 2, Figure S1, and Figure 2 show that regardless of tumor motion ranges, the dose distribution with the 30-mm collimator

has the highest γ passing rate in all criteria. With 10-mm tumor motion ranges, the γ passing rates of plans using the 30-mm collimator (M2_1 and M2_2) were above 95% in γ (5%/3 mm), even above 90% in γ (3%/3 mm), only M2_2 failed to 87.65% in γ (2%/2 mm). But the γ passing rates of the plans using 20 mm or 20+35 mm (M1_1/M1_2/M3_1 and M3_2) were much lower, and the γ passing rates of M1_1 and M1_2 were less than 75% in γ (2%/2 mm) using the 20-mm collimator. With 30 mm tumor motion ranges, the γ passing rates using the 30-mm collimator (M5_1 and M5_2) were above 90% in γ (5%/3 mm) but failed in γ (3%/3 mm) and γ (2%/2 mm). The γ (5%/3 mm) passing rates of the plans using 20 mm or 20 + 35 mm (M4_1/M4_2/M6_1 and M6_2) were all failed. Especially, M6_2 using the 20+35 mm collimator was 63.92% in γ (5%/3 mm).

γ Analysis Results Between Different Tumor Motion Ranges

The γ (5%/3 mm) passing rates of the measured plan dose distribution of 10-mm tumor motion ranges (M1/M2/M3) were much higher than those of 30-mm tumor motion ranges (M4/M5/M6), while the other parameters reminded the same, as shown in Figure 2. The γ (5%/3 mm) passing rates of the measured plan dose distribution of 10 mm tumor motion ranges were all above 90% with different collimator sizes. But only the γ (5%/3 mm) passing rates of the measured plan dose distribution of 30-mm tumor motion ranges using the 30-mm collimator could keep above 90%, the 20 mm and 20 + 35 mm collimators both failed and were below 80%. The dose variances may come from the high-dose regions, in which the relative measured dose was higher than the relative calculated dose of the plan, as shown in Figure 3.

γ Analysis Results Between Different Prescriptions and Periods

γ (5%/3 mm) passing rates of M11 were all failed. The γ (5%/3 mm) passing rates of M5 were slightly higher than that of M11, suggesting that the prescription may not be the most important factor to impact dose accuracy. In spite of increasing the dose heterogeneous inside the PTV, the lower prescription isodose also increase the treatment time, it may not decrease the dose uncertainty when treating a large motion range tumor using XST. The γ (5%/3 mm) passing rates of M12 were nearly the same with that of M5, suggesting that the influence of periods of tumor motion may be also small.

γ Analysis Results Between Different Treatment Starting Phases

Among the measurements of the same plans which were treated with different starting phases, the γ passing rates of static measurement (M7) were the best. The M5 with treatment starting phase at the end of exhale passed in both 2 measurements. The M8 with treatment starting phase at the midventilation: from

Table 2. γ Analysis Results in the Moving Target for Different Plan and Motion Parameters.

Measurement #	γ (3%/3 mm)	γ (2%/2 mm)	γ (5%/3 mm)	DD 5%	DD 3%	DTA 3 mm
M1(1) ^a	89.77%	67.28%	93.48%	90.75%	84.16%	78.15%
M1(2) ^a	90.29%	72.65%	95.61%	91.00%	84.45%	78.64%
M2(1)	99.41%	96.12%	99.84%	87.95%	83.48%	93.72%
M2(2)	93.01%	87.65%	96.37%	87.96%	83.84%	87.59%
M3(1)	91.33%	87.25%	92.92%	92.27%	89.58%	86.64%
M3(2)	88.87%	80.92%	91.54%	91.36%	88.03%	78.42%
M4(1)	72.80%	57.67%	78.24%	81.82%	75.37%	68.52%
M4(2)	65.32%	46.11%	71.05%	81.23%	74.87%	60.06%
M5(1)	86.42%	69.96%	91.22%	84.69%	75.83%	80.06%
M5(2)	94.74%	80.37%	97.46%	85.08%	76.13%	89.47%
M6(1)	77.90%	56.53%	81.58%	86.64%	78.06%	70.58%
M6(2)	52.73%	45.67%	63.92%	82.83%	76.80%	52.60%
M7(1)	99.35%	96.65%	99.51%	86.10%	77.65%	96.90%
M7(2)	98.03%	91.92%	99.84%	85.84%	76.91%	91.33%
M8(1)	77.42%	62.54%	82.34%	84.33%	75.66%	68.73%
M8(2)	82.75%	66.02%	87.86%	89.86%	81.75%	73.01%
M9(1)	91.65%	76.19%	95.13%	85.43%	76.81%	81.62%
M9(2)	84.35%	63.57%	88.35%	74.01%	66.57%	70.98%
M10(1)	87.77%	73.94%	90.68%	85.28%	76.58%	78.49%
M10(2)	82.85%	64.93%	86.89%	84.71%	76.18%	73.14%
M11(1)	75.81%	56.71%	81.14%	71.89%	65.66%	67.37%
M11(2)	84.84%	64.00%	88.12%	72.21%	65.49%	70.85%
M12(1)	94.67%	80.84%	95.77%	85.51%	76.73%	82.00%
M12(2)	89.41%	70.65%	92.82%	85.30%	76.45%	77.50%

Abbreviations: DD, dose difference; DTA, distance to agreement.

^aM1(1) means the first measurement result of M1group; M1(2) means the second measurement result of M1group.

exhale to inhale both failed in 2 measurements. The M9 with treatment starting phase at the midventilation: from inhale to exhale failed in 1 of 2 measurements. The M10 with treatment starting phase at the end of inhale also failed in 1 of 2 measurements. As shown in Figure 4, the γ passing rates of M5/M8/M9/M10 were variable. The unstable results of measurements at different treatment starting phases may indicate that the temporal interplay effect has a major impact on dose accuracy in XST.

Discussion

In this study, we investigated the feasibility of SBRT for lung tumors using CyberKnife XST for setup and static tracking. The static tracking method requires an ITV to account for the respiration-induced organ motion. The motion effect on the tumor dose was measured and evaluated with Gafchromic EBT3 films using a lung phantom consisting of a moving target and a static spine structure.

With 30-mm collimator plans, the measured dose passed the criteria γ (5%/3 mm) in all tumor motion ranges. But the γ passing rates of the plans using 20 mm or 20+35 mm were much lower than that with 30-mm collimator, especially with the 30-mm tumor motion range. This result suggested that the large collimators may be better for treating the moving lung tumors with XST than the small collimators.

The measured dose of small tumor motion ranges all passed the 90% criteria of γ (5%/3 mm), the results being much better

than those of large tumor motion ranges. This is consistent with the result of Chan *et al*, who found that the average DD was about 3.5% for small motion (10 mm SI motion) and up to 7.0% for large motion (20-mm SI motion) with a 5-mm ITV-to-PTV margin.¹⁷ These results suggest that the small tumor motion range (less than 10 mm) may reduce the gradient interplay effect.

The temporal interplay effect of treatment starting phase was an influencing strong factor of the dose accuracy of XST treatment since the dose passing rates of the same plan delivered at different starting phases showed great variation. Given that it originates from the tumor motion and beam delivery sequences, temporal interplay effect could not be overcome by choosing small movement tumors to treat. Although we consider the results from 10-mm tumor motion ranges as acceptable, we should also keep in mind that patients will not breathe as regularly as a moving phantom. Moreover, there are other factors, such as the change in breathing pattern or the baseline shift, which may introduce an additional temporal interplay effect and dose uncertainty to the delivery of CyberKnife SBRT with XST.

With static tumor tracking such as XST, dose blurring of respiratory motion is serious since the tumor moves while it not being tracked by the treatment beams.⁹ As shown in Figure 3, dose blurring was centered at the PTV, although their absolute dose did not vary considerably. However, the DTA was not coincident. These dose distribution discrepancies can be explained by the large dose gradients (eg, 25%-40%) inside the

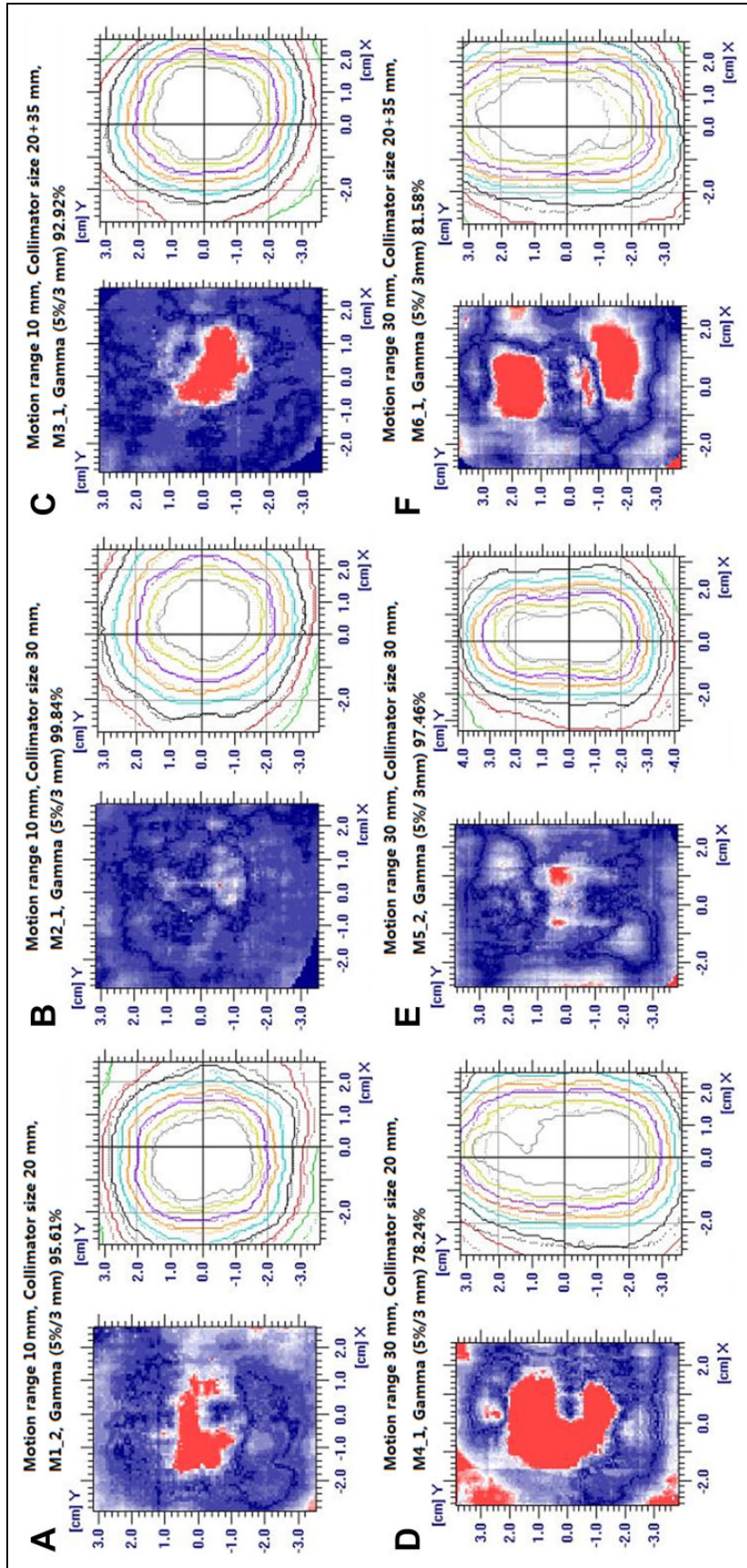


Figure 2. The γ (5%/3 mm) distribution and overlaid measured (thick solid line) and calculated (thin dotted line) isodose lines are shown for M1_2 [(A), motion range 10 mm, collimator size 20 mm]; M2_1 [(B), motion range 10 mm, collimator size 30 mm]; M3_1 [(C), motion range 10 mm, collimator size 20+35 mm]; M4_1 [(D), motion range 30 mm, collimator size 20 mm]; M5_2 [(E), motion range 30 mm, collimator size 30 mm]; M6_1 [(F), motion range 30 mm, collimator size 20+35 mm].

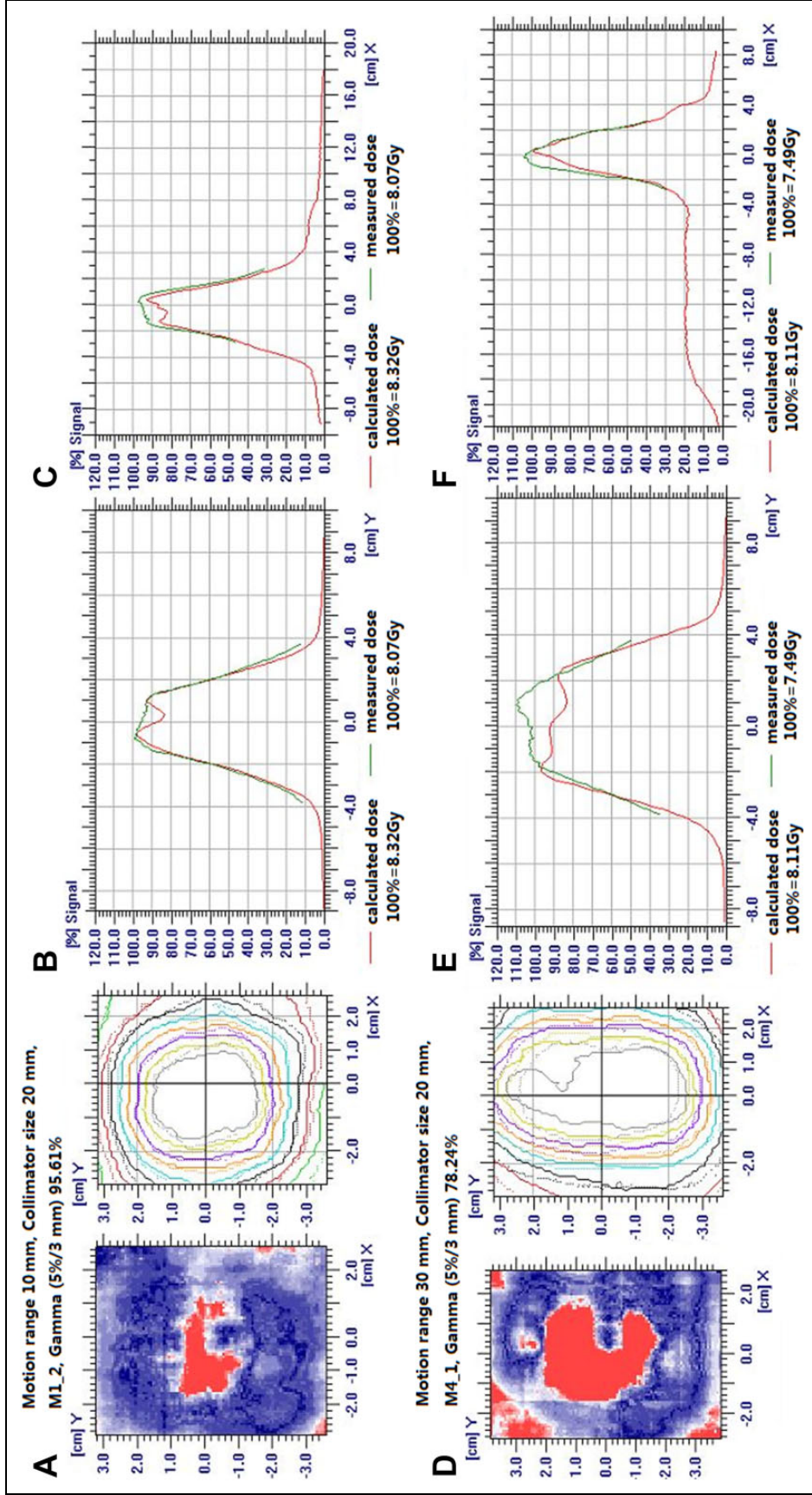


Figure 3. The γ (5%/3 mm) distribution and overlaid measured (thick solid line) and calculated (thin dotted line) isodose lines are shown for M1_2 (A) and M3_1 (D). Calculated and measured dose profiles corresponding to the thick solid line and thin dotted line in (A) and (D) are plotted in (B), (C), (E), and (F).

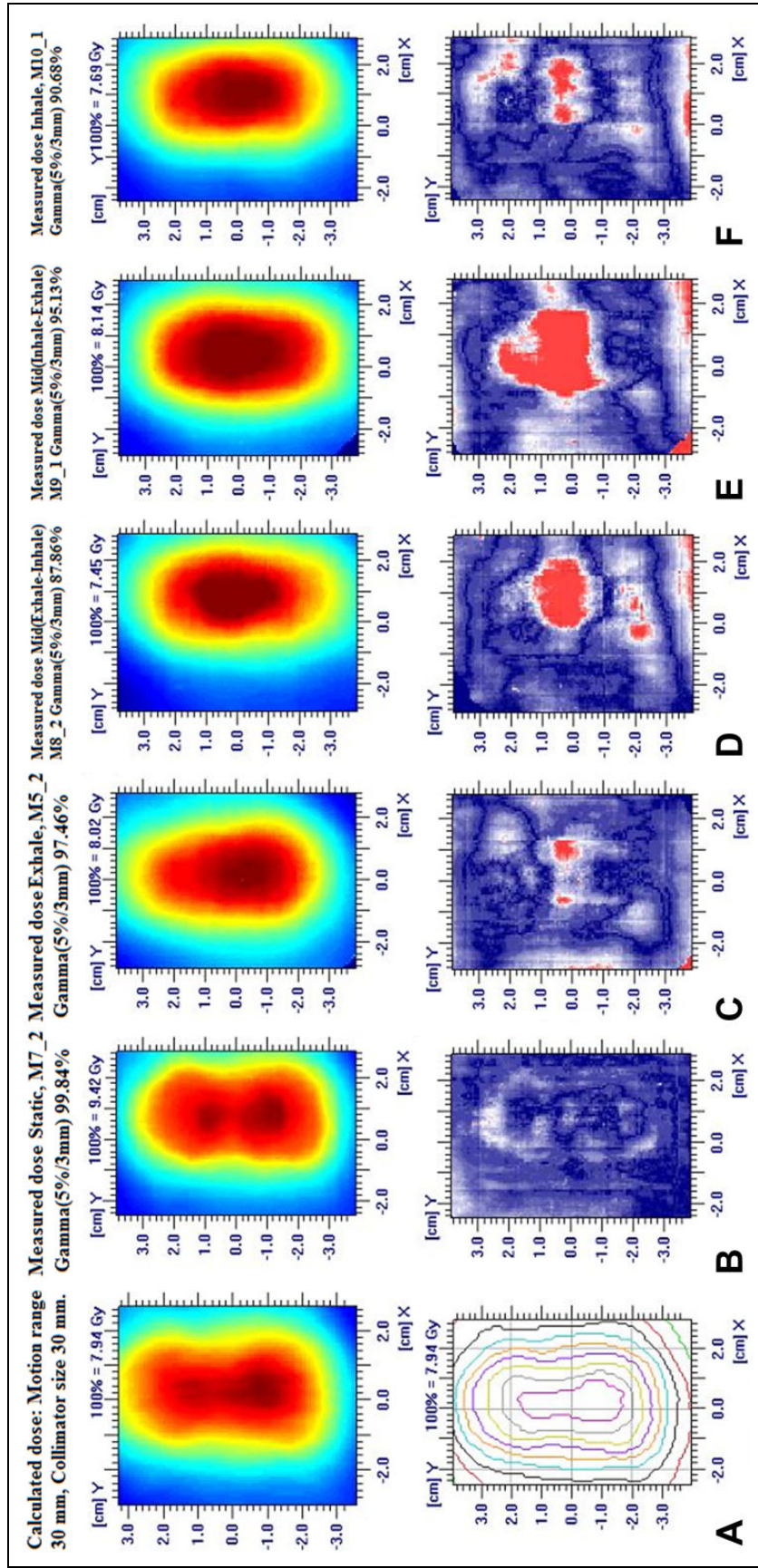


Figure 4. The γ passing rates of different treatment starting phases are shown. (A) shows the original plan dose distribution. The static result (B) is better than the other dynamic results (C-E and F).

PTV. This was in contrast to the 3D conformal radiotherapy or IMRT, where the dose blurring effect of tumor motion is generally pronounced at the field edge, but negligible at the center of PTV, which was covered with the uniform dose.

The limitations of the static tracking are obvious. First, due to the use of ITV, a large volume of normal tissues are exposed to the high-dose radiation. Second, since both the translational and rotational errors are calculated based on the spine alignment results, tracking accuracy is reduced for targets that are far away from the spine. Third, due to the unpredictable changes in the tumor motion during treatment, especially when the tumor is sometimes adjacent to the mediastinum and heart, the appropriate ITV-to-PTV margins is difficult to estimate. Since the tracing errors were significantly higher for tumors at a longer distance from the aligned center,⁴ the distance between the target and the imaging center should be considered cautiously when using XST for alignment. And an addition ITV-to-PTV margin and the tumor deformation evaluation are still needed to overcome the unpredictable variations in tumor motions and deformations.²³

There are some limitations of this study. Firstly, the phantom moved only in the SI direction; therefore, it did not represent the real situation of a patient's respiration. Since we try to evaluate the parameters that could influence the dose accuracy of the XST treatment, the single-direction motion was helpful with respect to eliminating interference of the other errors, such as setup errors and registration errors of x-ray images. Secondly, the target-to-spine distance in the phantom was relatively large, as this technique is aimed for tumors in the immediate vicinity of the spinal column. Since the phantom is rigid and the substitute tumor moves regularly, the degree of this impact may be reduced.

Conclusion

The large collimator size and small tumor motion range could reduce the gradient interplay effect of tumor motion in lung cancer SBRT. However, the temporal interplay effect of tumor motion in lung cancer SBRT delivered has a major impact on dose accuracy in XST. The XST technique should be used with caution in lung cancer SBRT because the interplay effect might be significant.

Authors' Note

Yu Chang and Hong-Yuan Liu contributed equally to this work. This study did not require an ethical board approval because it did not contain human or animal trials.

Declaration of Conflicting Interests

The author(s) declared no potential conflicts of interest with respect to the research, authorship, and/or publication of this article.


Funding

The author(s) disclosed receipt of the following financial support for the research, authorship, and/or publication of this article: This work was supported by the National Natural Science Foundation of China (grant no. 81803047), the Fundamental Research Funds for the Central

Universities (2019kfyXKJC061) and the National Key R&D Program of China (nos. 2016YFC0106701 and 2016YFC0106705).

ORCID iD

Gang Liu  <https://orcid.org/0000-0003-3510-3854>

Zhi-Yong Yang  <https://orcid.org/0000-0002-2806-1214>

Supplemental Material

Supplemental material for this article is available online.

References

1. Nuyttens JJ, van de Pol M. The CyberKnife radiosurgery system for lung cancer. *Expert Rev Med Devic.* 2012;9(5):465-475.
2. Bibault J-E, Prevost B, Dansin E, Mirabel X, Lacomberie T, Lartigau E. Image-guided robotic stereotactic radiation therapy with fiducial-free tumor tracking for lung cancer. *Radiat Oncol.* 2012;7(1):102.
3. Bhagat N, Fidelman N, Durack JC, et al. Complications associated with the percutaneous insertion of fiducial markers in the thorax. *Cardiovasc Inter Rad.* 2010;33(6):1186-1191.
4. Descovich M, McGuinness C, Kannarunimit D, et al. Comparison between target margins derived from 4DCT scans and real-time tumor motion tracking: insights from lung tumor patients treated with robotic radiosurgery. *Med Phys.* 2015;42(3):1280-1287.
5. Ho AK, Fu D, Cotrutz C, et al. A study of the accuracy of CyberKnife spinal radiosurgery using skeletal structure tracking. *Oper Neurosurg.* 2007;60(suppl 2):ONS-147-ONS-156.
6. Blot V, Coutand P, Malet C, Ayadi-Zahra M. Accuracy evaluation of the dose delivered by the three tracking modes of the CyberKnife™ Lung Optimized Treatment (LOT). *Physica Medica.* 2015;31(suppl 2):e25.
7. Stroom JC, Heijmen BJ. Geometrical uncertainties, radiotherapy planning margins, and the ICRU-62 report. *Radiation Oncol.* 2002;64(1):75-83.
8. Jiang SB, Pope C, Al Jarrah KM, Kung JH, Bortfeld T, Chen GT. An experimental investigation on intra-fractional organ motion effects in lung IMRT treatments. *Phys Med Biol.* 2003;48(12):1773.
9. Bortfeld T, Jokivarsi K, Goitein M, Kung J, Jiang SB. Effects of intra-fraction motion on IMRT dose delivery: statistical analysis and simulation. *Phys Med Biol.* 2002;47(13):2203.
10. Richter A, Wilbert J, Flentje M. Dosimetric evaluation of intra-fractional tumor motion by means of a robot driven phantom. *Med Phys.* 2011;38(10):5280-5289.
11. Nakamura M, Miyabe Y, Matsuo Y, et al. Experimental validation of heterogeneity-corrected dose-volume prescription on respiratory-averaged CT images in stereotactic body radiotherapy for moving tumors. *Med Dosim.* 2012;37(1):20-25.
12. Huang L, Park K, Boike T, et al. A study on the dosimetric accuracy of treatment planning for stereotactic body radiation therapy of lung cancer using average and maximum intensity projection images. *Radiation Oncol.* 2010;96(1):48-54.
13. Chen H, Wu A, Brandner ED, et al. Dosimetric evaluations of the interplay effect in respiratory-gated intensity-modulated radiation therapy. *Med Phys.* 2009;36(3):893-903.

14. Riley C, Yang Y, Li T, Zhang Y, Heron DE, Huq MS. Dosimetric evaluation of the interplay effect in respiratory-gated RapidArc radiation therapy. *Med Phys*. 2014;41(1):011715.
15. Chan MK, Kwong DL, Ng SC, Tong AS, Tam EK. Experimental evaluations of the accuracy of 3D and 4D planning in robotic tracking stereotactic body radiotherapy for lung cancers. *Med Phys*. 2013;40(4):041712.
16. Chan MK, Kwong DL, Ng SC, Tong AS, Tam EK. Accuracy and sensitivity of four-dimensional dose calculation to systematic motion variability in stereotactic body radiotherapy (SBRT) for lung cancer. *J Appl Clin Med Phys*. 2012;13(6):303-317.
17. Chan MK, Kwong DL, Lee VW, Leung RW, Wong MY, Blanck O. Feasibility study of robotic hypofractionated lung radiotherapy by individualized internal target volume and XSight spine tracking: a preliminary dosimetric evaluation. *J Cancer Res Ther*. 2015;11(1):150.
18. Yang Z-Y, Chang Y, Liu HY, Liu G, Li Q. Target margin design for real-time lung tumor tracking stereotactic body radiation therapy using CyberKnife XSight Lung Tracking System. *Sci Rep-UK*. 2017;7(1):10826.
19. Iwata H, Inoue M, Shiomi H, et al. Evaluation of dose uncertainty to the target associated with real-time tracking intensity-modulated radiation therapy using the CyberKnife Synchrony system. *Technol Cancer Res T*. 2016;15(1):101-106.
20. Wilcox EE, Daskalov GM. Evaluation of GAFCHROMIC[®] EBT film for CyberKnife[®] dosimetry. *Med Phys*. 2007;34(6):1967-1974.
21. Wilcox EE, Daskalov GM. Accuracy of dose measurements and calculations within and beyond heterogeneous tissues for 6MV photon fields smaller than 4 cm produced by CyberKnife. *Med Phys*. 2008;35(6):2259-2266.
22. Dieterich S, Cavedon C, Chuang CF, et al. Report of AAPM TG 135: quality assurance for robotic radiosurgery. *Med Phys*. 2011;38(6):2914-2936.
23. Yang Z, Chang Y, Brock KK, et al. Effect of setup and inter-fraction anatomical changes on the accumulated dose in CT-guided breath-hold intensity modulated proton therapy of liver malignancies. *Radiother Oncol*. 2019;134:101-109.